

## SUPPLEMENTAL MATERIAL

### Bypassing Dynamical Freezing in Artificial Kagome Ice

V. Schánilec,<sup>1,2</sup> B. Canals,<sup>1</sup> V. Uhlíř,<sup>2</sup> L. Flajšman,<sup>2</sup> J. Sadílek,<sup>2</sup> T. Šíkola,<sup>2,3</sup> and N. Rougemaille<sup>1</sup>

<sup>1</sup> *Univ. Grenoble Alpes, CNRS, Grenoble INP, Institut NEEL, 38000 Grenoble, France*

<sup>2</sup> *Central European Institute of Technology, CEITEC BUT,*

*Brno University of Technology, Purkyňova 123, Brno 612 00, Czech Republic*

<sup>3</sup> *Institute of Physical Engineering, Faculty of Mechanical Engineering,*

*Brno University of Technology, Technická 2, Brno, 616 69, Czech Republic*

(Dated: July 22, 2020)

#### MICROMAGNETIC SIMULATIONS

The micromagnetic simulations were performed using the Mumax3 code [1]. The nanomagnets are 750-nm-long, 250-nm-wide and 5-, 10- or 25-nm-thick. The depth of the notch is varied between 50 and 300 nm. The top angle made by the triangular shape of the notch is fixed to 30°. The considered material is permalloy: the exchange stiffness is set to 10 pJ/m, the magnetocrystalline anisotropy is neglected, and the spontaneous magnetization is  $8 \times 10^5$  A/m. The damping coefficient is set to 0.5. The mesh size has been reduced to  $2 \times 2 \times t$  nm<sup>3</sup> ( $t = 5, 10, 25$ ) to limit the influence of numerical roughness.

#### ADDITIONAL MEASUREMENTS

In the following, we provide additional measurements supporting those presented in the main text.

##### Positioning the notches

The notch rule introduced in this work allows to imprint any desired configuration satisfying the ice rule. Each imprinted state is of course two times degenerate. The LRO ground state being ordered, the notch arrangement is periodic. Supp. Fig. 1(a) allows to visualize the position and orientation of the notches in that particular case. The same procedure can be applied to any other spin ice configuration. Supp. Fig. 1(b) provides an example for an SL2 microstate.

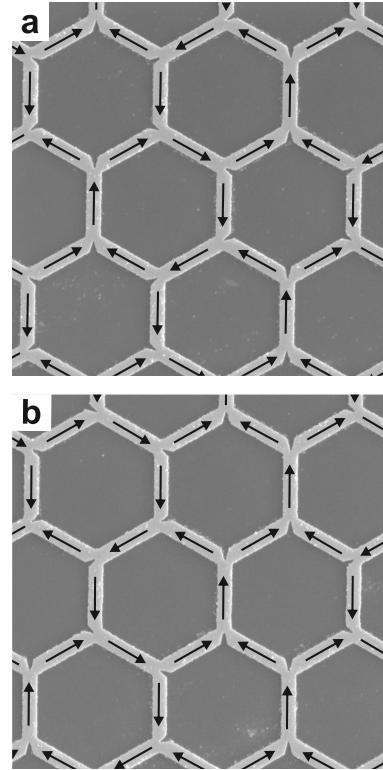


FIG. 1. Electron micrographs of two lattices showing the positions of the notches to imprint an LRO configuration (a) and an SL2 microstate (b). In the former case, the notches are periodically arranged since the LRO state is ordered. This is not the case for a spin disordered, but charge ordered SL2 microstate. The arrows illustrate one of the two possible imprinted spin states. The field of view is  $6 \times 6 \mu\text{m}$ .

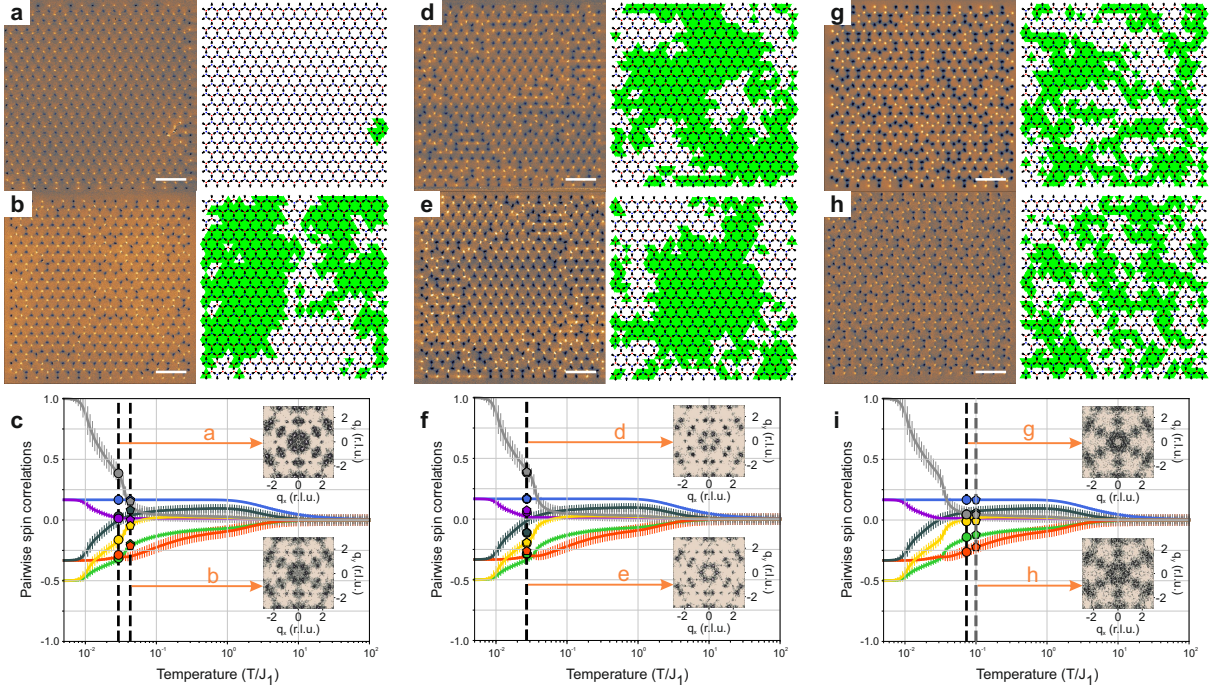


FIG. 2. Magnetic images with their associated spin-charge representation (a,b,d,e,g,h), and analysis of the pairwise spin correlations (c,f,i). Three cases are considered: 1) An imprinted SL2 microstate (a-c) obtained for lattices fabricated with 200 nm (a) and 150 nm (b) notches, 2) An imprinted LRO microstate (d-f) in two different, but similar lattices, 3) An imprinted LRO microstate (g-i) for the same lattice demagnetized with a long (g) and short (h) field protocol. From the analysis of the spin correlations, an effective temperature can be deduced (c,f,i). The insets show the magnetic structure factors computed from the spin configurations. The fraction of vertices breaking the notch rule is <1% (a), 17% (b), 21% (d), 23% (e), 39% (g), and 39% (h).

### Imaging fragmented spin liquid microstates

In Figure 3 of the main text, we illustrate the impact of the notch size on the spin configuration obtained after a demagnetization protocol, when the LRO ground state is imprinted in the lattice. The results clearly show that large notches (200 nm) bring the system into the imprinted state, whereas smaller (100 nm) notches lead to a disordered magnetic state, with pairwise spin correlations compatible with those of the SL1 phase. Similar results are obtained when imprinting an SL2 microstate (see Supp. Fig. 2). When the notch size is large, about 200 nm, the imprinted state is reached after the demagnetization protocol [Supp. Fig. 2(a)]. For a smaller notch size, about 150 nm, crystallites of the SL2 state are observed [Supp. Fig. 2(b)]. Comparing the experimental values of the first seven spin-spin correlators with those predicted by the dipolar Kagome ice model, we find that the effective temper-

ature is only weakly affected by the notch size [Supp. Fig. 2(c)]. In both cases, the associated magnetic structure factors reveal the fingerprints of a fragmentation process: a disordered but structured diffuse background signal coexists with emerging Bragg peaks [see insets in Supp. Fig. 2(c)]. We note that emergent pinch points are observed for large notches, evidencing the presence of algebraic pairwise spin correlations.

### Reproducibility

Our findings have been obtained reproducibly, in several lattices. In Supp. Figs. 2(d), 2(e) and 2(f) we compare two different arrays with an imprinted LRO configuration. In both cases, the notch size is 200 nm, but the sample was field demagnetized for a shorter time compared to Fig. 3(b) in the main text (see also Supp. Figs. 2(g), 2(h) and 2(i) for

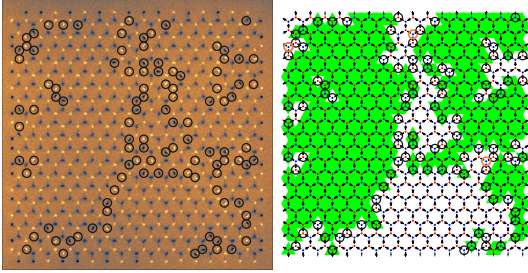


FIG. 3. Magnetic image with its associated spin-charge representation for an SL2 imprinted configuration. The circles indicate the position where the notch rule is not obeyed. These circles always belong to a domain wall, except a few cases (in orange in the spin-charge map) bridging two vertices violating the notch rule.

a comparison between two demagnetization times). Crystallites of the LRO ground state are observed, with charge domains spanning across the entire lattice [see Supp. Figs. 2(d) and 2(e)]. The analysis of the spin-spin correlations reveals that their associated effective temperatures, and thus their magnetic structure factors, are nearly identical [see Supp. Fig. 2(f)].

### Breaking the notch rule

In Figure 4(a) of the main text, we show that the notch rule is broken at the domain wall boundary separating LRO crystallites. Forming a domain wall thus induces an energy penalty proportional to the energy gap  $E_2 - E_1$  between the two vertex types. This observation is not specific to the case of LRO domain walls. A similar result is found in the case of charge domain walls separating SL2 phases, as illustrated in Supp. Fig. 3. Analyzing the entire image reveals that the notch rule is not obeyed within the domain walls (see the 108 circles within the spin-charge map). Except for a few instances, all the circles contain a vertex adjacent to a domain wall. Sometimes, the notch rule is broken close to the boundary of a domain, between two vertices violating the notch rule (see the three orange circles). However, the notch rule is never broken within the charge domains and essentially contributes to the domain wall energy.

## MONTE CARLO SIMULATIONS

Here, we examine the thermodynamics of the spin Hamiltonian describing our experimental system. The question we want to answer is to what extent the presence of the notches modifies the physics of the dipolar kagome ice. To do so, Monte Carlo simulations were performed using the Hamiltonian  $H = -\sum_{\langle i,j \rangle} J_{ij} \sigma_i \cdot \sigma_j$ , where  $\sigma_i$  and  $\sigma_j$  are Ising variables on the sites  $i$  and  $j$ . The  $\langle \rangle$  symbol means that only nearest neighbors are taken into account in the summation. We thus neglect further neighbor couplings and assume that the physics of the system is fully driven by the notches. Because the vertex symmetry is broken by the presence of the notches, two coupling strengths per vertex must be considered. We note  $J_2$  the coupling strength between the two nanomagnets sharing the notch, and  $J_1$  the two other coupling strengths. In all simulations,  $J_1$  is set to 1. The lattice is built as in the experiments: the notches (i.e., the  $J_1$  and  $J_2$  couplings) are placed in such a way that the target low temperature configuration is the LRO ground state of the dipolar kagome ice.

The Monte Carlo simulations were performed on  $18 \times 18 \times 3$  kagome lattice sites with periodic boundary conditions. A single spin flip algorithm is used. The system is cooled from  $T/J_1 = 100$  to the lowest possible temperature.  $10^4$  modified Monte Carlo steps (mmcs) are used for thermalization, where one mmcs corresponds to a set of local updates sufficiently long to achieve stochastic decorrelation.  $10^4$  mmcs measurements then follow the thermalization. The magnetic structure factor is composed of a  $81 \times 81$  matrix covering a  $\pm 3\pi$  area in reciprocal space. The specific heat, the entropy and the magnetic structure factors were calculated as a function of the normalized temperature  $T/J_1$ .

When  $J_2$  is substantially larger than  $J_1$ , i.e., when the notch size is large, Monte Carlo simulations reveal an ordering transition from a high temperature paramagnet to the target LRO microstate [see Supp. Fig. 4(a)]. These findings are consistent with what is observed experimentally when the notch size is large (200 nm). When  $J_2 = J_1 = 1$ , we recover the thermodynamic properties of the kagome Ising antiferromagnet [see Supp. Fig. 4(b)]. The thermodynamics of this model consists of two temperature regimes separated by a crossover [2–4]: a paramagnet at high temperature, and a spin liquid with exponentially decaying spin-spin correlations at low tem-

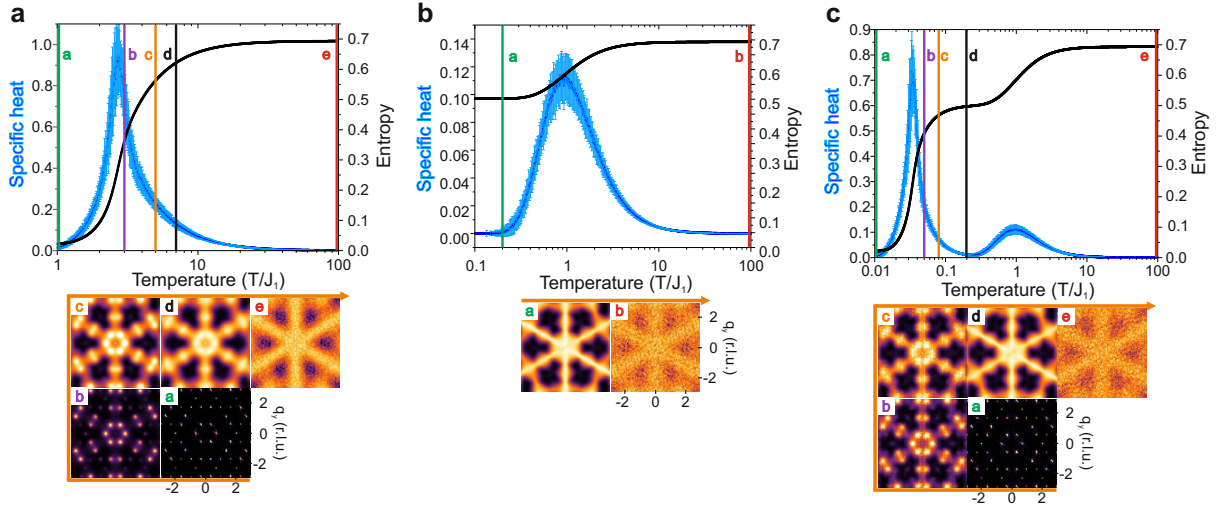


FIG. 4. Temperature dependence of the specific heat, entropy per site and magnetic structure factor when  $J_2 = 5$  (a),  $J_2 = 1$  (b), and  $J_2 = 1.05$  (c).  $J_1 = 1$  in all three cases.

perature. [5] An interesting situation occurs when  $J_2 \gtrsim J_1$ . For example, when  $J_2 = 1.05$  and  $J_1 = 1$ , the system is described by a crossover between a high temperature paramagnet and a spin liquid, followed by a phase transition leading to the target LRO microstate [see Supp. Fig. 4(c)]. The entropy per site thus shows a plateau at a value compatible with the 0.501 value expected for the short range kagome ice [5]. These results are consistent with the experimental observations when the notch size is small (100 nm).

As the ordering transition occurs, the magnetic structure factor reveals the existence of Bragg peaks together with a diffuse background signal (see Supp. Fig. 4(c) at  $T/J_1 \sim 0.05$ ). This map is reminiscent of the fragmented state observed in the dipolar kagome ice [6]. However, the magnetic structure factor does not show the pinch points associated with a fragmented Coulomb phase. Rather than a fragmented spin liquid (SL2), we observe here the formation of LRO crystallites embedded within a spin liq-

uid (SL1-like) as the phase transition is approached. In fact, the SL2 manifold is absent in our spin Hamiltonian, and the system crystallizes in a one-step process. This is a direct consequence of the absence of dipolar interactions in the short range spin Hamiltonian we consider.

- 
- [1] A. Vansteenkiste *et al.* AIP Advances **4**, 107133 (2014).
  - [2] I. Syozi, Prog. Theor. Phys. **6**, 306-308 (1951).
  - [3] K. Kano and S. Naya, Prog. Theor. Phys. **10**, 158-172 (1953).
  - [4] The kagome Ising antiferromagnet is equivalent to the short range kagome spin ice, where the frustration originates from the multiaxial Ising anisotropies and the ferromagnetic couplings between nearest-neighbours [see R. Moessner, Phys. Rev. B **57**, R5587-R5589 (1998)].
  - [5] A. S. Wills, R. Ballou and C. Lacroix Phys. Rev. B **66**, 144407 (2002).
  - [6] B. Canals *et al.* Nature Commun. **7**, 11446 (2016).